Int J Mater Form
DOI 10.1007/s12289-014-1183-x

ORIGINAL RESEARCH

Infrared heating assisted thermoforming of polypropylene clay nanocomposites

T. P. Mohan · K. Kanny

Received: 24 February 2014 / Accepted: 18 June 2014

Abstract The objective of this work is to study the influence of nanoclay addition in PP sheet during infrared (IR) heating assisted thermoforming process. The effect of nanoclay on viscoelastic, friction and dimensional characteristics during sheet forming was examined. The result indicated that the nanoclay addition improves the sagging (sagging depth and sagging disintegration) and plugging (plug depth and friction) properties during sheet forming. The plugging properties of nanoclay filled PP sheet resulted in the improved physical characteristics (minimal change in thickness (Δt) and % dimensional elongation) when compared with unfilled PP sheet. The nanoclay filled formed PP sheet resulted in improved tensile and dynamic mechanical properties when compared with unfilled formed PP sheet.

Keywords Thermoforming · Nano-structures · Mechanical properties · Physical properties · Thermoplastic resin

Introduction

Thermoforming is a process of making plastic objects from sheet or film using heat and pressure above glass transition temperature (T_g) or melting point (T_m) of a polymer [1, 2]. During heating the polymer softens due to their viscoelastic characteristics and when placed above the metal mold cavity with pressure (in the form of air pressure, vacuum or mechanical aid) followed by cooling forms desired products [3–5]. A wide range of products have been manufactured by thermoforming process from medical to electronic devices and with range of polymeric materials such as PP, HDPE, ABS, PVC and PS [6–10].

In general, thermoforming process takes place with plug assisted or vacuum assisted techniques [11, 12]. As the thermoforming process takes place at elevated temperature, it is one of the difficult processes to analyze, as it involves understanding of complex variables, such as viscoelastic characteristics of polymer, shear induced deformation and complex geometry of product shape. In previous works, the influence of thermoforming variables such as sheet/film temperature [13], plug material [14], plug temperature [15], plug rate [16], surface finish of the product [17], plug geometry [18], pressure [19] and viscoelastic behavior [20] of material were extensively analyzed. It was observed that most of these parameters were interdependent and one property influence other, and hence will be difficult to single out one parameter of influence. For example, the increase of temperature of processing affects the viscoelastic behavior of the material and which in turn affects the shear induced stretching of the sheet/film.

Looking at the sheet/film material itself, PP has made tremendous progress due to their availability, cost effectiveness, high thermal stability and favorable physical and mechanical properties. PP based trays are commonly used in food packaging and consumer applications, which are processed by thermoforming technique [21, 22]. However, in the recent past, many polymeric materials were being modified with additives and fillers. For example, a significant research works on polymer-clay nanocomposites (PCN) were carried out in recent past and various types of polymeric nanocomposites including PP were produced. The chemically treated montmorillonite (MMT) clays were filled into the PP polymer to enhance their thermal, mechanical and physical properties. The intercalation of polymeric matrix into the intergallery region of chemically treated clay nanolayers result in nanocomposite formation [23–26]. Even though hundreds of

T. P. Mohan · K. Kanny (✉)
Composites Research Group, Department of Mechanical Engineering, Durban University of Technology, Durban, South Africa
e-mail: kannyk@dut.ac.za

Published online: 27 June 2014

studies were carried out in PP nanoclay composites, the study on PP nanoclay based products are very much limited and detailed study is required in these subjects. For instance, Rund Abu-Zurayk et al. [27, 28] have carried out extensive study on the biaxial stretching property of polypropylene-clay based nanocomposites. It was observed that the delamination of nanoclay layers was increased due to stretching and the crystalline fraction of PP, tensile properties (strength, elongation and modulus) and dynamic mechanical properties (storage modulus and glass transition temperature, T_g) of the stretched sheets were increased due to the nanoclay addition. In another study, it was observed that the tensile property of nanoclay filled un-stretched sheet was lower, and it increased due to stretching at the stretch ratio of≥2.5. Tongchen et al. [29] observed shear induced crystallinity in nanoclay filled PP films up to 5 wt.%. The crystallinity increased up to 2 s^{-1} shear rate and beyond which the crystallinity is similar to that of neat PP film. Seyed and Abdellah [30] studied the PP-nanoclay film properties. Clay orientation and delamination along the flow direction of the film were observed with increased crystalline properties. About 25–40 % increased tensile modulus and with decreased oxygen permeability were observed. It was also observed that the rheological property of the formed PP nanocomposite film/sheet property is different to that of unformed film/sheet [31, 32]. From the literature, it was observed that the physico-chemical property of the unformed and formed film/sheet properties significantly changes, in which the latter was influenced by processing and product conditions. Therefore, the physical property of thermoformed sheet like thickness, dimensional elongation and tensile property were affected due to processing, nanoclay and viscoelastic behavior of the sheet/film material. It was observed that the effects of nanoclay on the physical property of the formed sheet were not fully understood or explored. A slight alteration of viscoelastic property of film/sheet due to nanoclay addition may significantly change the thermoformed product property. However, several researches on nanoclay affecting the viscoelastic characteristic of PP material was available [33–36]. Hence the objective of this work is to understand the effect of nanoclay on viscoelastic and physical properties of thermoformed PP trays. The influence of nanoclay on sagging and plugging properties during sheet forming were examined in this work. The sagging properties were studied by analyzing sagging depth at sheet forming temperature (140 °C) and disintegration and Dynamic Mechanical Analysis (DMA). The plugging properties were studied by analyzing coefficient of friction (μ), plug depth and physical properties due to plugging (i.e. % thickness variation and % elongation at different sections of formed tray).

Expertimental details

Materials

Polypropylene (PP) pellets of melting point 168 °C with melt flow index (MFI) of 10 g/10 min were procured from Chempro, South Africa. Cloisite® 30B nanoclay was used as filler in PP polymer and obtained from Southern Clay Products, USA. This clay is natural montmorillonite clay, which was organically modified with a quaternary ammonium salt. The organic modifier being MT2EtOH: methyl, tallow, bis-2-hydroxyethyl, quaternary ammomium, where T is Tallow (~65 % C18, ~ 30 % C16; ~ 5 % C14) with total modifier concentration of 90 meq/100 g clay.

Thermoforming

The thermoforming process consists of three main steps, and their sequence are represented in Fig. 1. The 1st step was compounding of PP pellets with nanoclay using REIFFENHAEUSER single screw extruder. The pellets and nanoclays were introduced at the hopper section of the extruder while the melt mixing took place at the screw section of the extruder. The extruder has a 40 mm diameter single rotating screw with a length/diameter ratio (L/D) of 24 and driven by a 7.5 kW motor. Three heating zones along the length of the extruder screw were maintained as follows: Zone 1 (Hopper or pellet loading end – 190 °C), Zone 2 (center region of screw – 230 °C) and Zone 3 (extrusion end – 230 °C), with constant screw speed of 60 rpm.

The 2nd step was sheet making of molten extrudate samples from extrusion. The molten extrudate (~20 g) was collected in an air pressure assisted flat plate die set-up maintained at 190 °C. The molten sample was immediately compression molded with an air pressure of 3 bars to form a flat 0.3 mm thick sheet. The flat sheet was then taken out; air cooled and cut into the dimensions of mold tray for thermoforming.

The 3rd step was the plug assisted thermoforming process of a tray. The sheet was heated by in-house build infrared (IR) heating and followed by plugging process. In this IR heating, the sheet was placed above the base mold and the top mold separately placed in the IR heating chamber until the sheet temperature reaches 140 °C. The IR heating was carried out using a panel heating system with medium IR wavelength (3.7 μm) operating at 15 wsi. The sheet temperature was precisely monitored by a non-contact temperature gun thermometer (MT697 series) supplied by Laboratory Supplies Co., South Africa. As soon as the sheet temperature reaches 140 °C, the softened sheet with mold was taken out and immediately plugged with top mold by air-pressure assisted set-up at 2 bar pressure to form a tray. The formed tray was removed from die and left aside for air cooling. The air-cooled tray was

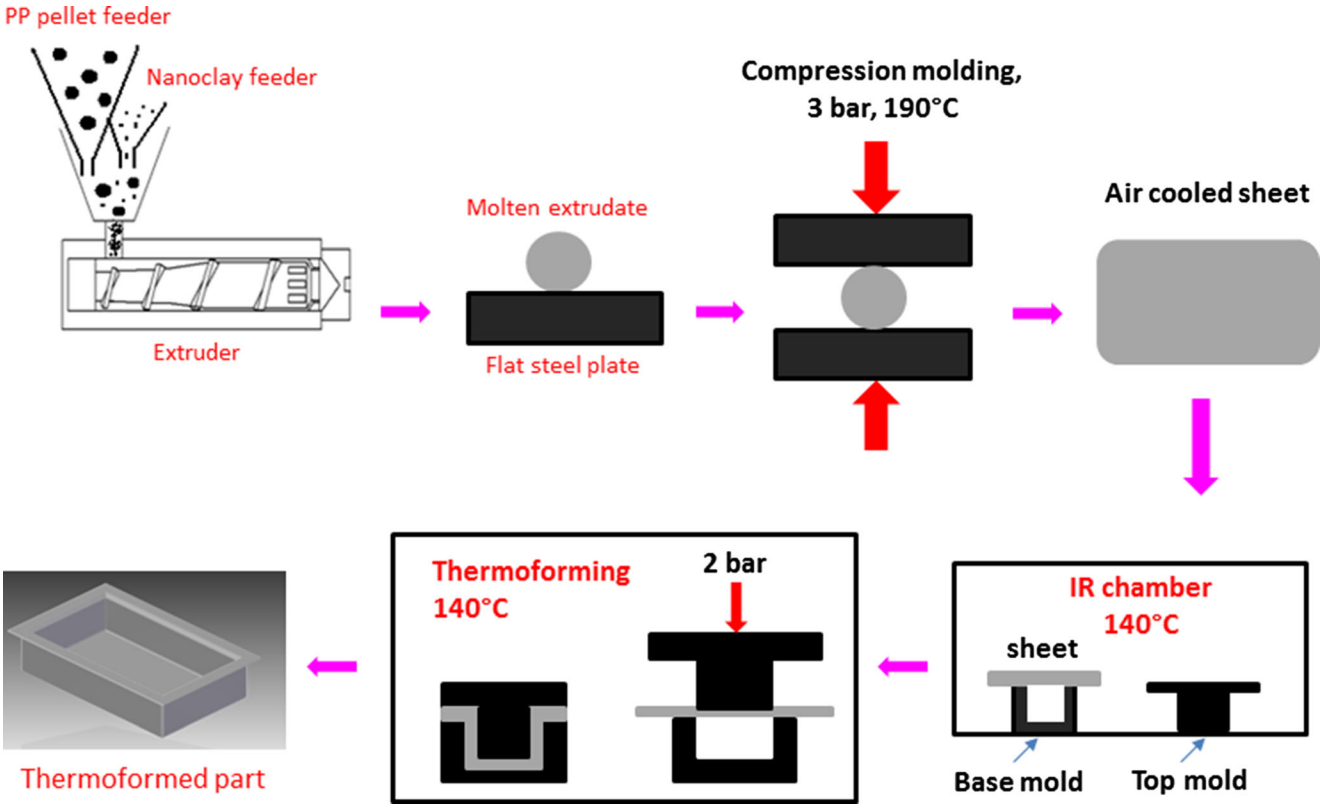

Fig. 1 Schematic of different steps of thermoforming

then trimmed across with flange section with a dimension of 5 mm, followed by characterization and testing. Plug assisted molds consists of a pair of steel base and top molds. The dimension of base mold cavity equal to the outer dimension of tray and dimension of top (plug) mold equal to the base mold cavity but with 0.3 mm lower than the dimension at all sides. A tray of length 50 mm, width 30 mm and height 15 mm were prepared from sheet by plug assisted molding.

Characterization and testing

The structure of sheet was studied by X-ray diffraction (XRD) and Transmission electron microscopy (TEM) methods. A Philips PW1050 diffractometer was used to obtain the X–Ray diffraction patterns using CuKα lines (λ=1.5406 Å). The diffractrograms were scanned up to 25° (2θ) in steps of 0.02° with a scanning rate of 0.5°/min. Microscopic investigations of selected sheet specimens at the various nanoclay weight compositions were conducted using a Philips CM120 BioTWIN transmission electron microscope operating at 20 to 120 kV. Thin section of a specimen was prepared using an LKB/Wallac Type 8801 with ultratome III 8802A Control Unit. Ultra-thin transverse sections, approximately 80–100 nm in thickness were sliced using a diamond coated blade.

Tensile tests on the un-stretched and stretched parts of unfilled and nanoclay filled PP tray specimens was carried out using the LLOYDS Tensile Tester fitted with a 20 kN load cell. The tensile tests of stretched part were performed along the transverse and longitudinal direction of stretching, at a crosshead speed of 1 mm/min in accordance with the ASTM D3039 standard with proper clamping at the end of test sheet. Five tensile specimens were taken, and the average value was considered for plotting stress–strain curve. It is envisaged that the standard deviation of all the test specimen values was within 3 %. The tensile specimens were obtained from the same location for all the unfilled and nanoclay filled sheet series. The tensile fracture surface morphology of test samples was examined by Zeiss Environmental Scanning Electron Microscopy (ESEM), operating at 20 kV. Dynamic mechanical analysis of the stretched sheet was carried out at a frequency of 10 Hz in a 3-point bending mode with cantilever clamps at ends using the TA instruments model Q800 from −20 to 150 °C under atmospheric conditions.

As soon as the temperature reached 140 °C the sheet started to sag and this was measured as sagging depth. To carry out this measurement, a sheet was kept above the base mold in IR chamber and heated up to 140 °C, followed by cold water quenching. The sagging depth was measured by measuring the distance from the neutral point of sheet before sagging. It was measured at the center point of the sheet where maximum sagging was noticed. When the sheet kept at 140 °C for prolonged period, the sagging was severe and the material starts to disintegrate. The sagging depth of respective sheets

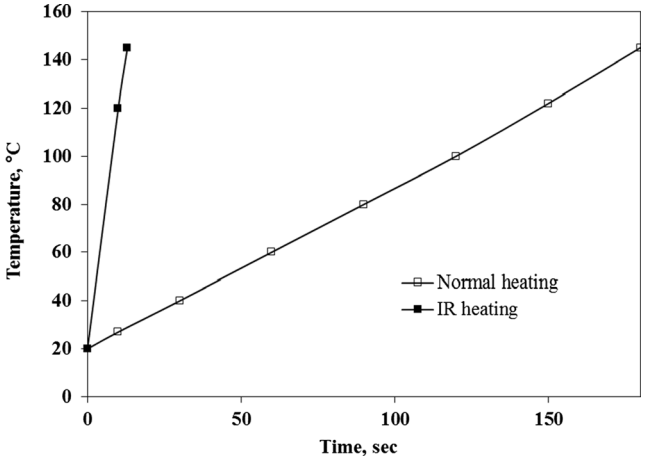

Fig. 2 Time-Temperature curve of normal convection heating and IR heating of PP sheets

during disintegration was also measured. To study the plugging property, the sheet was heated above the base mold in IR heating up to 140 °C. Then the top mold was plugged at 2 bars to measure the maximum vertical length that the sheet is stretched (plug depth). After this, the whole setup (base and top molds with sheet) was immediately removed and quenched in a cold-water mediums. The quenched sheet specimen was then taken out, and the plug depth was measured.

The dynamic coefficient of friction (μ) of sheet was measured as per Morales et al. model [37]. As there is no standard test procedure available to measure the dynamic coefficient of friction, a commonly well acceptable procedure was adopted in this study. In this method, the mobile steel block (the steel material that was used for thermoforming mold) with 5 cm × 5 cm × 5 cm dimension was placed on the sheet at one end, and the distance covered due to impact by a modified pendulum impact tester was measured, from which the μ was calculated as per Eq 1.

$$\mu = \frac{E_0 - E}{mgl} \tag{1}$$

where, μ is the dynamic coefficient of friction, E_0 energy of the pendulum when striking the mobile block, E the energy of the pendulum after striking the mobile block, m is the mass of the mobile block and l is the distance covered by the mobile block on the sheet (maintained at 140 °C) due to impact.

The physical property of the thermoformed tray was studied by measuring the dimensional elongation and % thickness variation of the formed sheet. These two parameters were measured at base, stretched thin wall and flange section of the thermoformed tray. To measure dimensional elongation, 2 points were marked at unformed sheet where the base, thin wall and flange section were going to be formed. The points were kept at same distance of 3 mm at all the sections (base, thin wall and flange). After thermoforming, the distances between 2 points were again measured at all the sections from which the dimensional elongation of formed sheet was calculated.

The thickness of unformed and formed sheet was measured using a micrometer. The thickness was measured at the flange, stretched wall and base section of the tray. Five readings were measured at each section, and average was discussed. The % dimensional elongation and % thickness variation was calculated as per the Eqs 2 and 3 respectively.

$$\%\ thickness\ variation = \frac{T_f - T_i}{T_i} \times 100 \tag{2}$$

$$\%\ dimensional\ elongation = \frac{L_f - L_i}{L_i} \times 100 \tag{3}$$

Where, T_i and T_f are the thickness of the sheet before and after forming respectively, L_i and L_f are the initial and final length of sheet before and after forming. The dimensional elongation and thickness that were measured at 3 different sections, namely, flange, stretched wall and base were numbered as measuring point 1, 2 and 3 respectively in discussing the result.

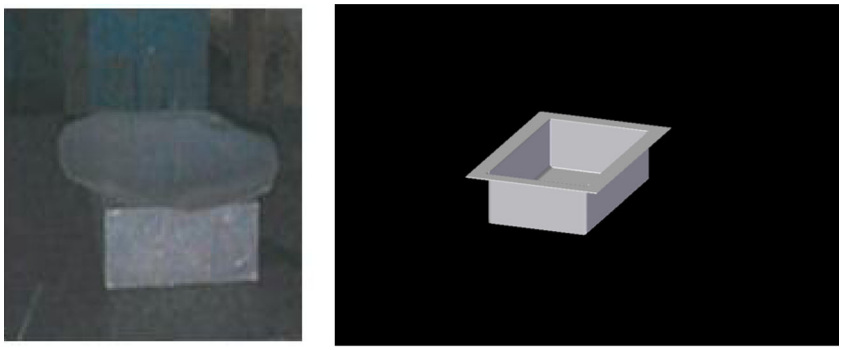

(a) **(b)**

Fig. 3 Representative image of (**a**) sagging of PP sheet during IR heating and (**b**) thermoformed sheet

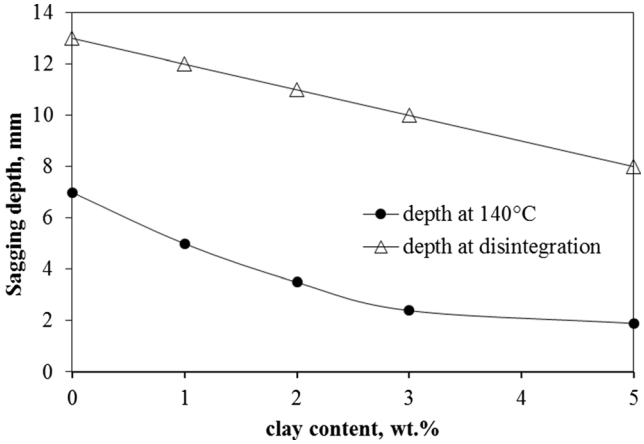

Fig. 4 Effect of nanoclay sagging depth of PP sheet series

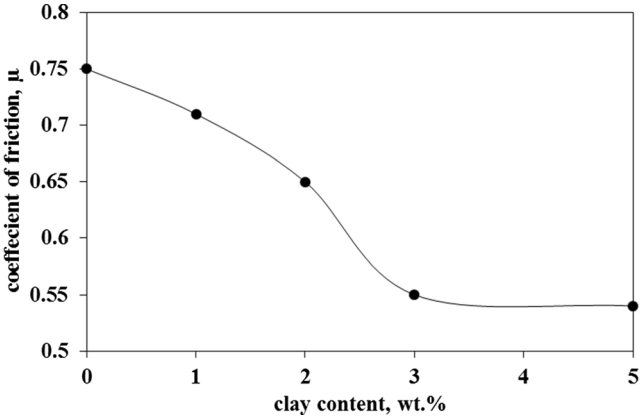

Fig. 6 Effect of nanoclay content on dynamic coefficient friction of PP sheet series

To compare the efficiency of IR heating over conventional convection heating, the PP sheet was placed in an oven maintained at 140 °C (Model 30GC, Quincy Lab, Inc. USA) operating at 1,200 W and the time required to reach 140 °C by PP sheet was monitored by temperature gun thermometer as discussed above.

Results and discussions

Thermoforming

Heating

One of the most important stages of thermoforming process of plastic sheets is the heating stage. The heating is required to reach the forming phase above T_g or T_m. The amount of heat energy required to reach forming phase for thermoforming sheets varies from polymer to polymer. In general, PP requires more amounts of heat energy than many other plastics materials (heat content of about 180 BTU/LB) to reach the forming phase [38]. Therefore, longer heating times are required to obtain thermoforming condition in PP based materials. However, by using IR based heating set-up, this heating time has been significantly reduced. IR generates huge amount of heat during processing, and to understand the advantage of IR heating over normal heating, a heating test was performed in a PP sheet as shown in Fig. 2 by measuring the time taken by the sheet to reach forming phase (140 °C). Clearly, it was observed that IR heating had shown about 14 times reduction in heating time (~180 s for normal convection heating and~13 s for IR heating) when compared to the conventional convection heating. This gives a huge advantage in production and processing of trays.

Sagging property

Figure 3 shows the schematic image of a PP sheet as soon as it reached forming temperature 140 °C (Fig. 3a) and a thermoformed tray (Fig. 3b). Sagging of PP sheet observed during processing (Fig. 3a) might be due to viscoelastic characteristics of polymer. To understand this sagging phenomenon with the influence of nanoclay in PP sheet, depth of sagging was measured as soon as the sheet reaches 140 °C and the result is shown in Fig. 4. Unfilled PP sheet shows sagging depth of 7 mm and they were continuously reduced as nanoclay content increased in the PP sheet. Maximum

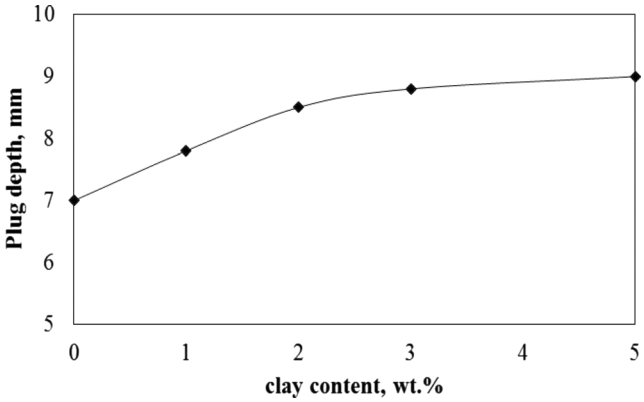

Fig. 5 Effect nanoclay on plug depth during sheet forming

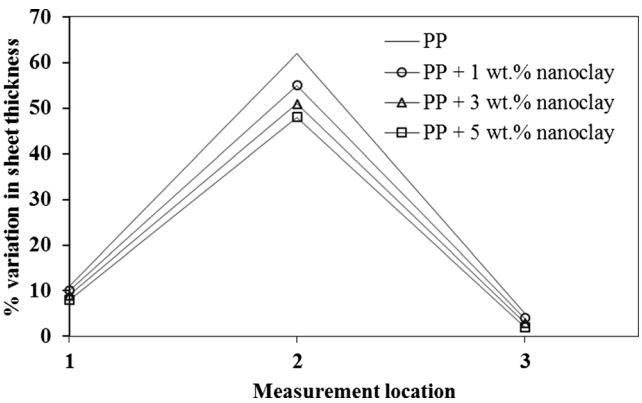

Fig. 7 Effect of nanoclay content on thickness of formed sheet

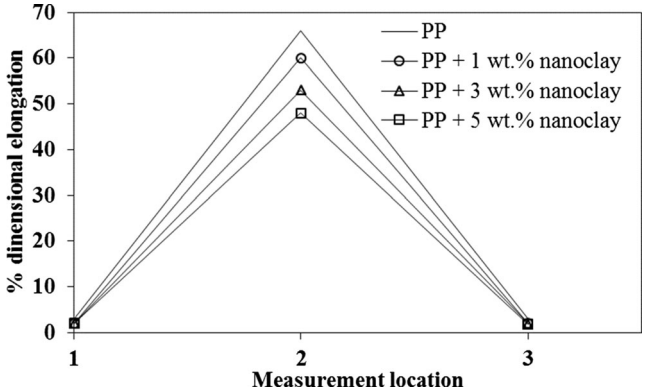

Fig. 8 Effect of nanoclay content on dimensional elongation of formed sheet

reduction in sagging depth was observed for 5 wt.% nanoclay filled PP sheet with sagging depth of 1.9 mm, a reduction of~ 73 % when compared with unfilled PP sheet.

When the sheet was maintained at this processing temperature (140 °C) for prolonged period the sagging was more severe and disintegrates leading to the failure of the material from processing. The influence of nanoclay on the sagging depth at disintegration was examined and the result is also shown in Fig. 4. Unfilled PP sheet shows sagging depth of 13 mm at disintegration, whereas it continuously reduced as nanoclay content increases in PP sheet. PP sheet with 5 wt.% nanoclay have shown maximum reduction in sagging depth of 8 mm, which is about 38 % lower than unfilled PP sheet.

The sagging can be due to the softness of the material [4, 19, 22] or materials own weight which allows excessive strains during high temperature processing [6]. As the temperature increases the softness also increases and thereby yields more which is what observed in unfilled PP sheet with high sagging depth. However, nanoclay filled PP have shown increased dynamic storage modulus as observed elsewhere [33–36] (and also discussed in "Dynamic mechanical analysis" section) even at elevated temperatures and this phenomenon could have resulted in reduction of sagging depth in the nanoclay filled sheet. This result suggests that the nanoclay addition increases the processing time window for sheet by reducing sheet sagging.

Plugging property

Plugging is an important property of sheet forming, and it determines the physical characteristics of the formed products. The influence of nanoclay on plugging properties was examined and Fig. 5 shows the plug depth during plugging of the unfilled and nanoclay filled PP sheet. Unfilled PP sheet shows plug depth of 7 mm, and it was continuously increased as nanoclay increased in PP sheet. PP with 5 wt.% nanoclay sheet shows plug depth of 9 mm, which is 28 % higher than that of unfilled PP sheet. The possible reason for the increased plug depth of nanoclay filled PP sheet could be due to the reduced friction between the metallic mold and polymer sheet during forming. Figure 6 shows the dynamic coefficient of friction (μ) of unfilled and nanoclay filled PP sheet series at 140 °C. Unfilled PP sheet shows μ of 0.75, and it continuously decreased as nanoclay content increased, and μ is 0.54 for 5 wt.% nanoclay filled PP sheet. The reduction of friction due to nanoclay addition in polymeric matrix composites was observed in earlier literatures [39–42]. It was also reported that decrease of polymeric sheet friction during processing will result in increased slippage between polymeric sheet and mold cavity, ultimately resulting in increased plug depth [37,

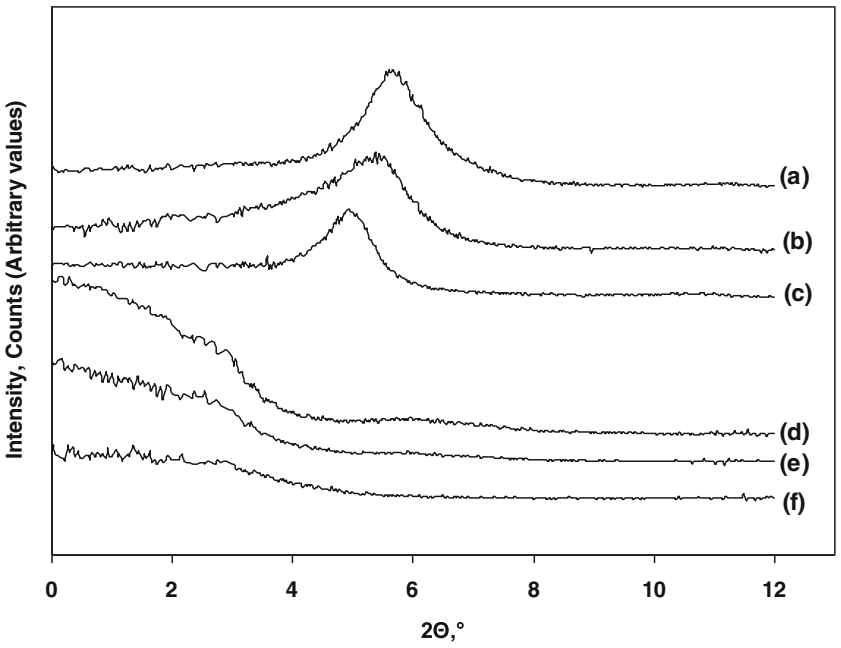

Fig. 9 XRD pattern of (**a**) Nanoclay, PP with (**b**) 5 wt.%, (**c**) 3 wt.%, (**d**) 2 wt.%, (**e**) 1 wt.% and (**f**) 0 wt.% nanoclay

43, 44]. In this study, it was observed that nanoclay filled PP reduces sheet friction and hence increases the plug depth by slippage between sheet and mold cavity. Due to the reduced friction of nanoclay filled sheets, it was expected to have better physical properties (i.e. minimal change in the thickness (Δt) and % dimensional elongation) when compared with the unfilled PP formed sheet.

To verify this phenomenon, thickness was measured at 3 measuring points of the formed sheet 1st point being the base section, 2nd point being the thin walled stretched section and the 3rd being the flange section of the formed sheet. The % increase of thickness (Δt) of the formed sheet with respect to unformed sheet was shown in Fig. 7. The result indicates that the stretched section of sheet shows the maximum change of Δt followed by base and flange section respectively. Large variation of Δt was observed in unfilled PP sheet when compared with nanoclay filled PP sheet. Continuous reduction of Δt was observed as nanoclay content continuously increased in PP sheet. This could be possibly due to the reduced μ along with favorable slippage, in which the polymeric sheet was able to form a product shape with minimal change in Δt thickness. Whereas, unfilled PP sheet had shown high friction and hence resulted in reduced slippage, due to which the sheets were plugged by high stretching and therefore affecting the thickness.

The effect of nanoclay on the dimensional elongation was observed, and the result was represented in Fig. 8. The dimensional elongation was maximum at the stretched section of the sheet. Unfilled PP sheet shows maximum elongation values when compared with nanoclay filled PP sheet. The dimensional elongation continuously reduces as nanoclay content increases in the PP sheet. The large elongation of unfilled PP sheet can be due to the increased friction. The increased friction has caused reduced slippage between unfilled PP sheet and metallic mold resulting the parts to form by stretching (resulting in high % dimensional elongation).

Structure and morphology

Figure 9 shows the XRD patterns of nanoclay, unfilled and nanoclay filled PP sheet series. Nanoclay shows a diffraction peak at 2θ of 5.72° and this corresponds to the interlayer distance or d-spacing (d) of nanoclay (001 plane) equal to 15.4 Å (calculated from Bragg's diffraction principle, $2d\text{-}\mathrm{Sin}\theta = n\lambda$, in which d is interlayer spacing, θ is the diffraction angle, n is the order of reflection and λ is the wavelength of X-ray used). XRD pattern of unfilled PP doesn't show any diffraction peak up to 2θ of 12°. PP with 5 wt.% nanoclay shows a diffraction peak at 2θ of 5.42°, which was lower than the diffraction angle for pure nanoclay. This result suggests that the nanolayers of clays in polymer matrix were expanded (i.e. the interlayer distance increased) as the interlayer distance (d) was equal to 16.3 Å. This increased interlayer distance (d) of clay could be possibly due to the polymer matrix. The matrix polymer had entered into the interlayer spacing of clay nanolayers during nanocomposite processing and could have increased the d-spacing/interlayer spacing of nanoclay. PP with 3 wt.% nanoclay also shows a diffraction peak, but with further reduced 2θ angle when compared with pure nanoclay and 5 wt.% nanoclay filled PP. The diffraction peak occurred at 2θ value of 5° and corresponds to interlayer distance (d-spacing) of 17.7 Å. This shows the interlayer distance of clay for the 3 wt.% nanoclay was further increased when compared with nanoclay and 5 wt.% nanoclay filled PP. This could be

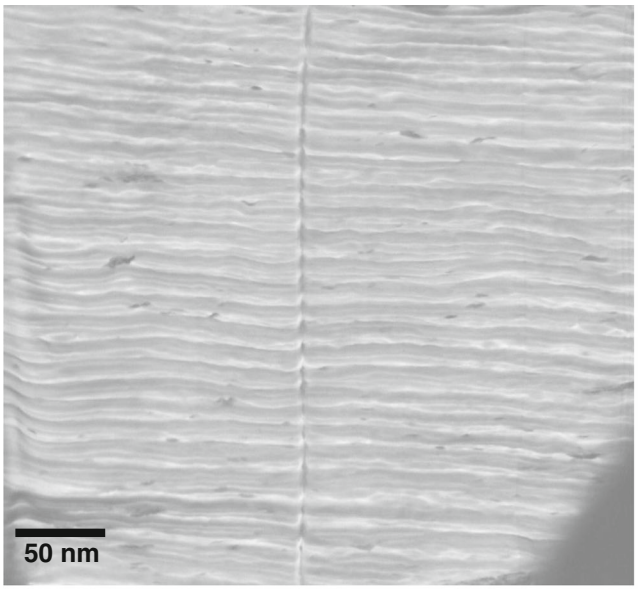

(a)

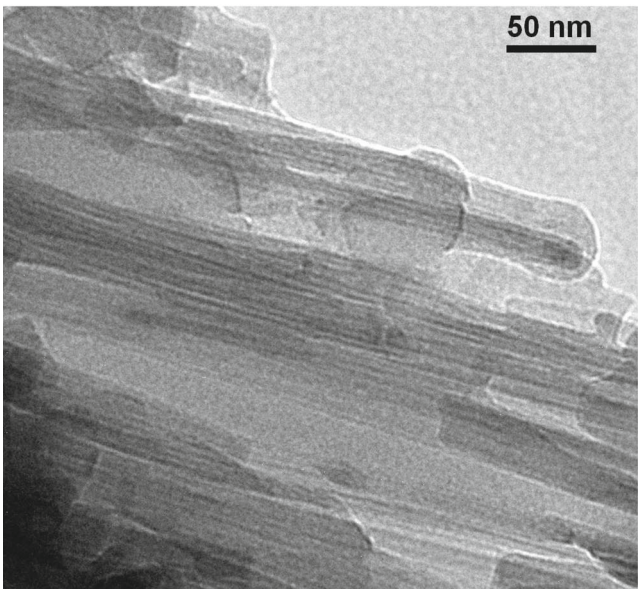

(b)

Fig. 10 TEM pictures of PP with (**a**) 2 wt.% and (**b**) 5 wt.% nanoclay content

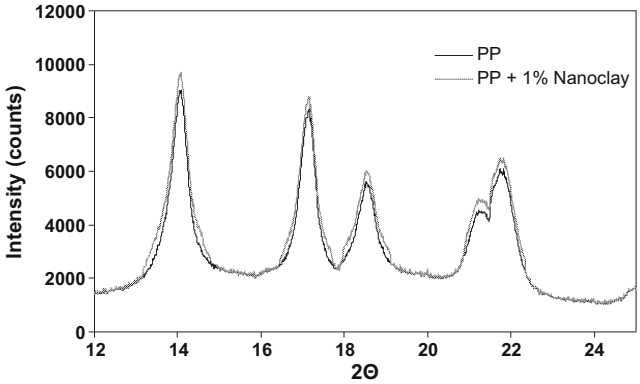

Fig. 11 Higher angle XRD patterns of PP and 1 wt.% nanoclay filled sheet before forming

possibly due to the presence of more amounts of PP matrix in the clay interlayer spacing in 3 wt.% nanoclay filled PP nanocomposites.

On the other hand, PP with 1 and 2 wt.% doesn't show any diffraction peak. This suggests that the nanolayers of clays were well separated to each other (>75 Å so that Bragg's diffraction law will not satisfy) or the nanolayers were randomly dispersed in the polymer matrix, in which the Bragg's diffraction cannot occur. Literature results show that the random (or well separated) dispersion of nanolayers of clay in the polymeric matrix is called as an exfoliated structure. Whereas ordered arrangement of clay nanolayers with increased interlayer spacing than neat nanoclay is called as an intercalated structure [23–26]. The exfoliated structure shows superior properties over an intercalated structure. In exfoliated structure, the nanolayers were individually dispersed with high contribution of an aspect ratio of clay nanolayer (length/thickness) compared with intercalated structure.

In this study, it was seen that nanoclay up to 2 wt.% in PP matrix resulted in exfoliated structure, and above that resulted in intercalated structure. Among the intercalated structures, the interlayer distance decreased as the nanoclay content increased from 3 to 5 wt.%. This result also shows that as

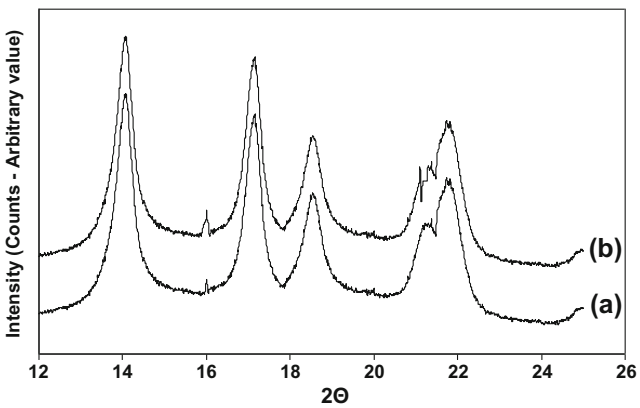

Fig. 12 XRD patterns of stretched part of (**a**) unfilled PP and (**b**) 1 wt.% nanoclay filled formed sheet

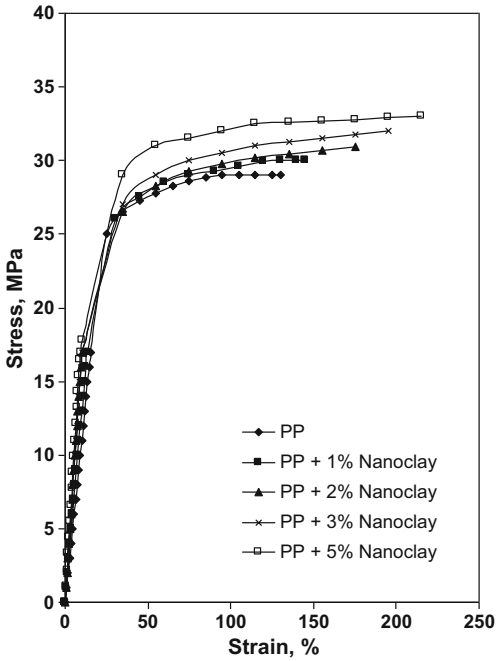

Fig. 13 Tensile stress – strain curves of unfilled and nanoclay filled formed sheet at transverse to stretch direction

the nanoclay content increases, it becomes difficult for PP matrix to intercalate into the intergallery region of nanoclays and induce exfoliated structure.

Figure 10 shows the TEM pictures of PP with 2 and 5 wt.% nanoclay. The nanolayers of clays were represented as dark phase while the matrix phase represented as a bright and continuous phase. TEM of 2 wt.% nanoclay filled PP shows relatively well separated nanoclay layers than that of 5 wt.%

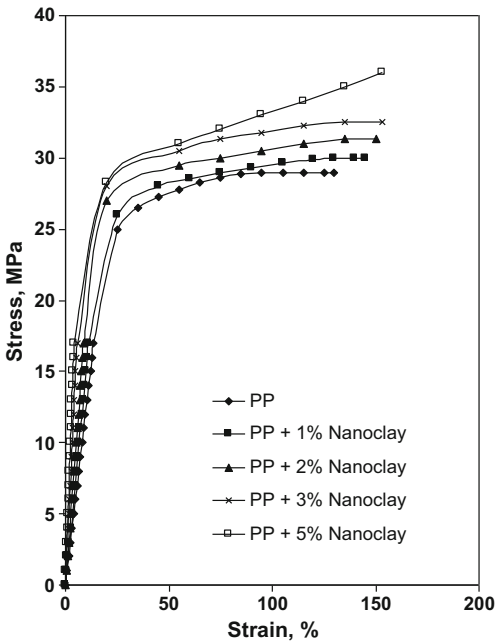

Fig. 14 Tensile stress – strain curves of unfilled and nanoclay filled formed sheet at longitudinal to stretch direction

Table 1 Tensile properties of stretched trays at transverse and longitudinal directions

Sheet Material	Tensile property along transverse direction to stretching						Tensile property along longitudinal direction to stretching					
	Modulus, GPa		Strength at break, MPa		Elongation at break, %		Modulus, GPa		Strength at break, MPa		Elongation at break, %	
	AVG	STD. DEV	AVG	STD. DEV	AVG	STD. DEV	AVG	STD. DEV	AVG	STD. DEV	AVG	STD. DEV
PP	1.1	0.13	29	1.5	130	5	1.25	0.11	29	1.2	130	5
PP+1 wt.% nanoclay	1.3	0.16	30	1.7	145	7	1.51	0.12	30	1.5	145	6
PP+2 wt.% nanoclay	1.2	0.15	32	1.6	175	6	1.93	0.12	32	1.3	150	8
PP+3 wt.% nanoclay	1.2	0.17	32	2.0	195	8	2.0	0.11	33	1.5	153	7
PP+5 wt.% nanoclay	1.2	0.17	33	1.5	215	7	2.1	0.13	36	1.4	153	6

nanoclay filled PP, indicating well separated nanolayers or exfoliated structure. PP with 5 wt.% nanoclay composites shows ordered arrangement of nanolayers resulting in intercalated structure. The TEM result also supports the XRD result of nanocomposite structure.

Figure 11 shows the higher angle XRD pattern of unfilled and 1 wt.% nanoclay filled PP composite. The result shows the diffraction peak of unfilled PP at 2θ value of 14.1°, 17°, 18.6°, 21.2° and 21.8°, and corresponds to the α crystalline (monoclinic) structure [45]. The XRD pattern of 1 wt.% nanoclay filled PP also shows similar α crystalline patterns of PP, however, with increased intensity values. This suggests the crystalline fraction of 1 wt.% nanoclay filled PP is higher than that of unfilled PP. The XRD result of nanoclay with other series (2 to 5 wt.%) also shows the same level of intensity peaks corresponding to 1 wt.% nanoclay filled PP (therefore, these peaks were not shown due to overlapping of curves). The Fig. 12 shows XRD patterns of unfilled and 1 wt.% nanoclay filled PP sheet at stretched section. Due to stretching new peaks were present at 2θ values of 16° and 21°. These new crystalline peaks were due to the β-phase (trigonal) PP structure [46]. Increased β phase intensity peaks were observed in 1 wt.% nanoclay filled PP, suggesting the nanoclay aid more β phase crystalline fraction during stretching. The literature results suggest that the β phase crystals were usually observed in PP under the influence of nucleating agents or stretching [46].

Tensile properties

The tensile properties of unfilled and nanoclay filled PP trays were evaluated along the transverse and longitudinal direction to the stretching, and these stress–strain curves were shown in Figs. 13 and 14 respectively, and the tensile properties were shown in Table 1. The tensile modulus along the transverse direction to stretching was increased in nanoclay filled PP trays. Maximum increase in modulus of 18 % was observed in 1 wt.% nanoclay filled PP tray over unfilled PP tray and there after continuously reduced to 9 % for 5 wt.% nanoclay filled tray. Tensile strength continuously increased as nanoclay content increased, and maximum increase of 14 % was observed in 5 wt.% nanoclay filled PP tray. Elongations at break values were continuously increased as nanoclay content increased. Maximum increase of elongation at break value of~ 1.65 times was observed in 5 wt.% nanoclay filled PP tray.

Table 2 Tensile properties of unformed sheet, formed sheet at flange and base sections

Material	Unformed sheet						Flange section of formed sheet						Base section of formed sheet					
	Modulus, GPa		Strength at break, MPa		Elongation at break, %		Modulus, GPa		Strength at break, MPa		Elongation at break, %		Modulus, GPa		Strength at break, MPa		Elongation at break, %	
	Avg.	Std. Dev.	Avg.	Std. Dev.	Avg.	Std. Dev.	Avg.	Std. Dev.	Avg.	Std. Dev.	Avg.	Std. Dev.	Avg.	Std. Dev.	Avg.	Std. Dev.	Avg.	Std. Dev.
PP	1	0.11	26	2	137	6	1	0.10	26	2	137	5	1	0.09	26	1	137	6
PP+1 wt.% nanoclay	1.1	0.10	27	2	141	5	1.1	0.12	27	3	141	5	1.1	0.11	27	3	141	5
PP+2 wt.% nanoclay	1.2	0.13	29	2	137	7	1.2	0.11	29	2	137	6	1.2	0.10	29	2	137	7
PP+3 wt.% nanoclay	1.2	0.12	30	3	130	6	1.2	0.12	30	2	130	5	1.2	0.11	30	2	130	4
PP+5 wt.% nanoclay	1.2	0.11	31	3	126	5	1.2	0.10	31	3	126	7	1.2	0.11	31	3	126	5

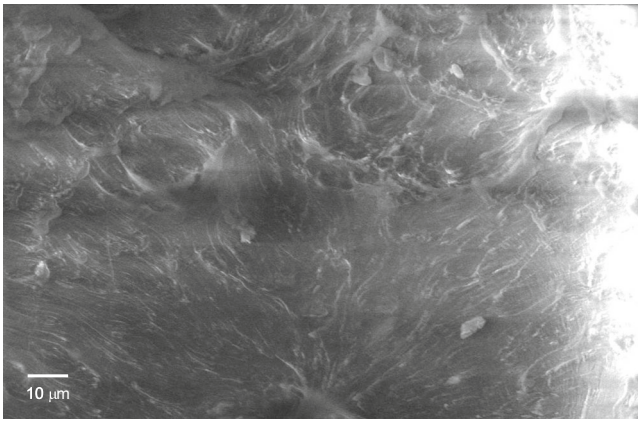

Fig. 15 Tensile fracture surface of 1 wt.% nanoclay filled formed PP sheet along the longitudinal to stretch direction

Similar increases in strain values of stretched sheet were also observed elsewhere [27, 47–49].

The tensile property of unfilled and nanoclay filled trays was different when measured along longitudinal to the stretch direction. Tensile modulus and strength were significantly increased, and it continuously increased as the nanoclay content continuously increased. Maximum increase of 68 % tensile modulus, 24 % tensile strength and 1.17-time elongation at break was observed in 5 wt.% nanoclay filled PP stretched sheet when compared with unfilled PP stretched sheet. However, % increase of elongation at break was less in longitudinal direction when compared with transverse direction of stretched sheet.

The tensile properties of unformed sheet and un-stretched section of formed sheet (i.e. flange and base section of a thermoformed tray) were also evaluated, and the values were shown in Table 2. The result shows the tensile properties of all these sheets (unformed, flange and base) were almost same. However, nanoclay filled sheet increases the tensile strength and modulus the PP sheet, with elongation at break values

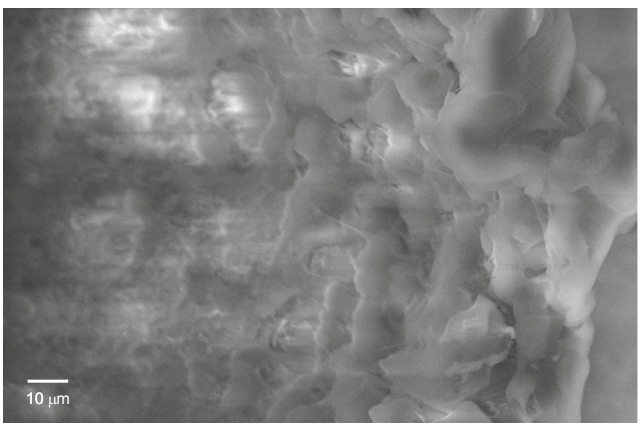

Fig. 16 Tensile fracture surface of 1 wt.% nanoclay filled formed PP sheet along the transverse to stretch direction

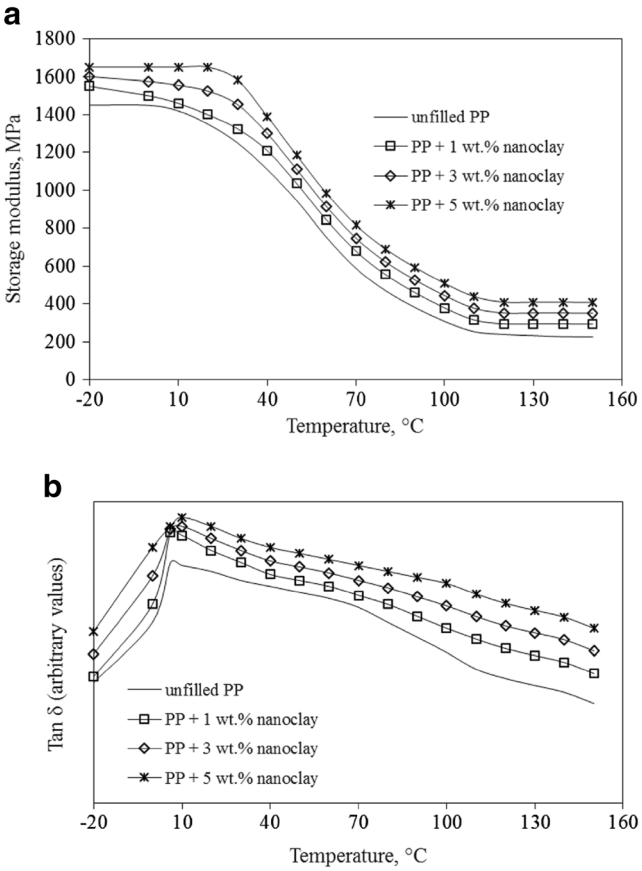

Fig. 17 Effect of nanoclay on (**a**) storage modulus and (**b**) Tan δ of PP sheet series

shows decreasing trend due to nanoclay addition. However, the elongation at break of stretched section of the formed sheet shows increasing trend due to nanoclay addition, which could be possibly due to the improved deformation mechanism due to nanoclay particles as reported elsewhere [27, 47–49].

In general, the improved tensile property of filled sheet is due to the nanoclay particles that were being dispersed at nanolevel. The hard ceramic phase of nanoclay has a tensile modulus of~165 GPa and hence resulted in improved modulus of nanoclay filled PP trays. Also there might be a deformation induced mechanisms like, crack pinning, particle pull-out, particle-polymer interface interactions, etc. [50, 51] due to nanodispersed clay particles resulting increased tensile strength. The significant increase of modulus and strength values along the stretch direction can be also due to β-phase crystalline structure during stretching. However, in transverse direction of tensile measurement, the nanoclay in amorphous polymeric phase might have resulted in increased strength and modulus values when compared with unfilled PP sheet. To some extent, these observations were observed in SEM analysis of fracture surface of tensile samples (Figs. 15 and 16). A cleavage and brittle type failure were observed along the stretch direction, with a significant amount of crystalline

phase (bright flake like regions). However, the tensile fracture surface along the transverse to stretch direction shows extended deformation and with plastic type failure, suggesting the amorphous phase had induced extended deformation before failure. Table 1 also shows that the rate of the increase of tensile properties were reduced in composites with>2 wt.% nanoclay composite. This can be due to the morphology of the nanoclay particles in the polymeric matrix. Up to 2 wt.% nanoclay in PP, exfoliated structures were observed and above 2 wt.% nanoclay in PP, intercalated structures were observed. In the exfoliated structure, the rate of the increase of tensile properties is higher when compared with intercalated structure. Even though intercalated structure shows increased tensile properties in absolute values, the rate of the increase was lower when compared with exfoliated structure. The increased values could be due to high nanoclay content (in which the property of clay contributing to composites increases due to higher concentration), whereas, decreased rate of the increase of value could be due to the intercalated structure. In the intercalated structure, the group of stack of clay nanolayers orient in particular direction and therefore, reduce the net aspect ratio of clay (length/thickness of nanolayer).

Dynamic mechanical analysis

The DMA was studied due to the clay addition significantly affecting the viscoelastic properties of the sheet during forming, particularly sheet sagging and disintegration. The DMA is the measure of storage modulus and Tan δ as a function of temperature, which are related to the viscoelastic characteristics of the polymer. Figure 17 shows the effect of nanoclay on the storage modulus and Tan δ of PP sheet at various temperatures. The result indicates that the storage modulus continuously increases as nanoclay content increases in PP sheet, and also at all temperature ranges. At 140 °C, the storage modulus of PP sheet series were 226 MPa, 294 MPa, 351 MPa and 404 MPa for unfilled PP, 1, 3 and 5 wt.% nanoclay filled PP sheet respectively. In Fig. 17b, the maximum value of Tan δ corresponds to the glass transition temperature (T_g) of the polymer. PP shows T_g of 5 °C and continuous increase of T_g was observed due to nanoclay addition in PP sheet. 5 wt.% nanoclay filled PP sheet shows T_g of 10 °C. Nanoclay is a hard ceramic material which has significantly higher modulus (~165 GPa) than that of PP (~1 GPa), therefore the composite has shown improved modulus when compared with PP matrix [52, 53]. Due to the hard phase of the nanoclay, the clay possibly arrests the movement of amorphous molecules of PP by increasing the T_g. This higher modulus of nanoclay filled composite series could have possibly improved the sheet sagging and disintegration properties during forming.

Conclusions

The objective of this work is to study the effect of nanoclay addition on viscoelastic properties during sheet forming. To carry out this study, 0 to 5 wt.% nanoclay were filled in PP followed by sheet making and thermoforming. The result indicated that the IR heating assisted thermoforming process was efficient and significantly reduced the heating time by about 14 times than that of normal heating methods. The viscoelastic results show that the nanoclay addition decreases sagging depth, increases the sagging disintegration and hence processing window.

The reduced dynamic coefficient of friction of nanoclay filled sheet resulted in improved plugging with better physical properties (i.e. thickness distribution and dimensional elongation) of thermoformed parts. Nanoclay addition beyond 5 wt.% was not carried out due to the difficulties in sheet forming and decreased rate of the increase of tensile properties due to intercalated structure.

Structural and morphological examination of unfilled and nanoclay filled PP composites shows the formation of exfoliated structure up to 2 wt.% nanoclay and above that shows the formation of intercalated nanocomposite structure. XRD results show the presence of α-phase crystalline structure of PP in un-stretched sheet, and stretched sheet shows both the presence of α-phase and β-phase crystalline structures. The nanoclay addition increases the crystalline fraction of PP structure in both stretched and un-stretched sheet. The tensile properties of nanoclay filled PP formed sheets was better than that of unfilled PP formed sheets.

Acknowledgments The authors acknowledge the support by the National Research Foundation (NRF) of South Africa [Grant No: 71599, Postdoctoral Fellowship]; and Postgraduate Research Assistance from Durban University of Technology, South Africa.

References

1. Ashter SA (2014) The Thermoforming Process. In: Ebnesajjad S (ed) Thermoforming of Single and Multilayer Laminates - Plastic Films Technologies, Testing and Applications. William Andrew imprint of Elsevier, Oxford, pp 13–38
2. O'Connor CPJ, Martin PJ, Menary G (2012) Viscoelastic material models of polypropylene for thermoforming applications. Int J Mater Form 3:599–602
3. Choo HL, Martin PJ, Harkin-Jones EMA (2008) Measurement of heat transfer for thermoforming simulations. Int J Mater Form 1: 1027–1030
4. Karamanou M, Warby MK, Whiteman JR (2006) Computational modelling of thermoforming processes in the case of finite viscoelastic materials. Comp Meth App Mech Eng 195:5220–5238
5. Ahzi, Puissant S (2007) Thermoforming process of amorphous polymeric sheets: modeling and finite element simulations. J App Poly Sci 106:1718–1724

6. Sala G, Di Landro L, Cassago D (2002) A numerical and experimental approach to optimize sheet stamping technologies: polymers thermoforming. Mater Dsg 23:21–39
7. Billon N (2008) Constitutive model for HIPS in the thermoforming range. Int J Mater Form 1:679–682
8. Yamaguchi M, Suzuki K-I (2002) Enhanced strain hardening in elongational viscosity for HDPE/crosslinked HDPE blend. II Processability of thermoforming. J App Polym Sci 86:79–83
9. Ashton JH, Mertz JAM, Harper JL, Slepian MJ, Mills JL, McGrath DV, Vande Geest JP (2011) Polymeric endoaortic paving: mechanical, thermforming, and degradation properties of polycaprolactone/polyurethane blends for cardiovascular applications. Acta Biomater 7:287–294
10. Stephenson MJ, Ryan ME (1997) Experimental study of the thermoforming of a blend of styrene-butadiene copolymer with polystyrene. Polym Eng Sci 37:450–459
11. Bhattacharyya D, Bowis M, Jayaraman K (2003) Thermoforming woodfibre-polypropylene composite sheets. Comp Sci Tech 63:353–365
12. Hosseini H, Vasilivich BB, Mehrabani-Zeinabad A (2006) Rheological modeling of plug-assist thermoforming. J App Polym Sci 101:4148–4152
13. Lee JK, Virkler TL, Scott CE (2001) Influence of initial sheet temperature on ABS thermoforming. Polym Eng Sci 41:1830–1844
14. Walczyk DF, Yoo S (2009) Design and fabrication of a laminated thermoforming tool with enhanced features. J Manf Process 11:8–18
15. Jagger RG, Okdeh A (1995) Thermoforming of polymethyl methacrylate. J Pros Dent 74:542–545
16. Hossini H, Berdyshev BV, Mehrabani-Zeinabad A (2006) A solution for warpage in polymeric products by plug-assisted thermoforming. Euro Poly J 42:1836–1843
17. Torres FG, Bush SF (2000) Sheet extrusion and thermoforming of discrete long glass fibre reinforced polypropylene. Comp Part A: App Sci Man 31:1289–1294
18. Molnár P, Ogale A, Lahr R, Mitschang P (2007) Influence of drapability by using stitching technology to reduce fabric deformation and shear during thermoforming. Comp Sci Tech 67:3386–3393
19. Warby MK, Whiteman JR, Jian W-G, Warwick P, Wright T (2003) Finite element simulation of thermoforming processes for polymer sheets. Math Comp Siml 61:209–218
20. O'Connor CPJ, Menary G, Martin PJ, McConville E (2008) Finite element analysis of the thermoforming of polypropylene. Int J Mater Form 1:779–782
21. O'Connor CPJ, Martin PJ, Sweeney J, Menary G, Caton-Rose P, Spencer PE (2013) Simulation of the plug-assisted thermoforming of polypropylene using a large strain thermally coupled constitutive model. J Mater Proc Tech 213:1588–1600
22. Ming-Meng P, Meng-Yan P, Wen-Shyang C, Zainal A, Mohd I (2014) Carbon footprint calculation for thermoformed starch-filled polypropylene biobased materials. J Clean Prod 64:602–608
23. Kiliaris P, Papaspyrides CD (2010) Polymer/layered silicate (clay) nanocomposites: an overview of flame retardancy. Prog Polym Sci 35:902–958
24. Xidas PI, Triantafyllidis KS (2010) Effect of the type of alkylammonium ion clay modifier on the structure and thermal/mechanical properties of glassy and rubbery epoxy-clay nanocomposites. E Polym J 46:404–417
25. Meneghetti P, Qutubuddin S (2006) Synthesis, thermal properties and applications of polymer-clay nanocomposites. Therm Acta 442:74–77
26. Kim TK, Kim BK, Kim YS, Ya L, Cho SY, Lee YB, Cho JH, Kim HMJ (2008) Properties of reactive hot melt adhesives modified by polyurethane containing PEG segment intercalated in sodium montmorillonite. Int J Mat Form 1:615–618
27. Abu-Zurayk R, Harkin-Jones L, McNally T, Menary G, Martin P, Armstrong C, McAfee M (2009) Biaxial deformation behavior and mechanical properties of a polypropylene/clay nanocomposite. Comp Sci Tech 69:1644–1652
28. Abu-Zurayk R, Harkin-Jones E, McNally T, Menary G, Martin P, Armstrong C, McAfee M (2010) Structure–property relationships in biaxially deformed polypropylene nanocomposites. Comp Sci Tech 70:1353–1359
29. Sun T, Chen F, Dong X, Zhou Y, Wang D, Han CC (2009) Shear-induced orientation in the crystallization of an isotactic polypropylene nanocomposite. Polym 50:2465–2471
30. Tabatabaei SH, Abdellah A (2011) Structure-oreintation-properties relationships for polypropylene nanoclay composite films. J Plas Film Sheet 27:87–115
31. Kashyap MJ, Ghosh AK (2013) Processing, rheology and characterization of polypropylene nanocomposites and their blown films. J Plas Film Sheet 29:228–248
32. Mirzadeh A, Kokabi M (2007) The effect of composition and draw-down ratio on morphology and oxygen permeability of polypropylene nanocomposite blown films. E Polym J 43:3757–3765
33. Feng-Hua S, Yan J-H, Huang H-X (2011) Structure and melt rheology of long-chain branching polypropylene/clay nanocomposites. J App Poly Sci 119:1230–1238
34. Hambir S, Bulakh N, Jog JP (2002) Polypropoylene/clay nanocomposites: effect of compatibilizer on thermal, crystallization and dynamic mechanical behaviour. Polym Eng Sci 42:1800–1807
35. Hong CK, Kim M-J, Oh SH, Lee Y-S, Nah C (2008) Effects of polypropylene-g-(maleic anhydride/styrene) compatibiizer on mechanical and rheological properties of polypropylene/clay nanocomposites. J Ind Eng Chem 14:236–242
36. Drozdov AD, Høg Lejre A-L, Christiansen J dC (2009) Viscoelasticity, viscoplasticity and creep failure of polypropylene/clay nanocomposites. Comp Sci Tech 69:2596–2603
37. Morales RA, Candal MV, Santana OO, Gordillo A, Salazar R (2014) Effect of the thermoforming process variables on the sheet friction coefficient. Mater Dsgn 53:1097–1103
38. Throne J (2011) Thermoforming. In: Kutz M (ed) Applied Plastics Engineering Handbook: Processing and Materials. William Andre imprint of Elsevier, Oxford, pp 333–358
39. Finney Charles R, Gnanamoorthy PR (2010) Rolling contact fatigue behavior of polyamide clay reinforced nanocomposite - effect of load and speed. Wear 269:565–571
40. Bhuyan S, Sundararajan S, Lu Y, Larock RC (2010) A study of the physical and tribological properties of biobased polymer–clay. Wear 268:797–802
41. Jawahar P, Gnanamoorthy R, Balasubramanian M (2006) Tribological behavior of clay-thermoset polyester nanocomposites. Wear 261:835–840
42. Dayma N, Satapathy BK, Patnaik A (2013) Structural correlations to sliding wear performance of PA-6/PP-g-MA/nanoclay ternary nanocomposites. Wear 271:827–836
43. Morales RA, Candal MV (2006) Diseño y fabricación de un molde de termoformado utilizando herramientas CAD/CAE. Revista de la Facultad de Ingeniería de la UCV 21:83–100
44. Chen S-C, Huang S-T, Lin M-C, Chein R-D (2008) Study on the thermoforming of PC films used for in-mold decoration. Int Comm Heat Mass Trns 35:967–973
45. Patil N, Invigorito C, Gahleitner M, Rastogi S (2013) Influence of a particulate nucleating agent on the quiescent and flow-induced crystallization of isotactic polypropylene. Polym 54:5883–5891
46. Mollova A, Androsch R, Mileva D, Gahleitner M, Funari SS (2013) Crystallization of isotactic polypropylene containing beta-phase nucleating agent at rapid cooling. E Polym J 49:1057–1065

47. Fermino DM, Parra DF, Oliani WL, Lugao AB, Diaz FRV (2013) HMSPP nanocomposite and Brazilian bentonite properties after gamma radiation exposure. Rad Phy Chem 84:176–184
48. Cauvin L, Kondo D, Brieu M, Bhatnagar N (2010) Mechanical properties of polypropylene layered silicate nanocomposites: characterization and micro–macro modelling. Poly Test 29:245–250
49. Lai SM, Chen WC, Zhu XS (2009) Melt mixed compatibilized polypropylene/clay nanocomposites: part 1 – the effect of compatibilizers on optical transmittance and mechanical properties. Comp: Part A App Sci Man 40:754–765
50. Mohan TP, Ramesh Kumar M, Velmurugan R (2006) Mechanical and barrier properties of epoxy polymer filled with nanolayered silicate clay particles. J Mater Sci 41:2929–2937
51. Bureau MN, Ton-That M-T, Perrin-Sarazin F (2006) Essential work of fracture and failure mechanisms of polypropylene-clay nanocomposites. Eng Frac Mech 73:2360–2374
52. Mohan TP, Kanny K (2010) Using image analysis for structural and mechanical characterization of nanoclay reinforced polypropylene composites. Engg 2:802–812
53. Lu HB, Nutt S (2003) Restricted relaxation in polymer nanocomposites near the glass transition. Macromol 36:4010